# Glutathione and phytochelatins jointly allow intracellular and extracellular detoxification of cadmium in the liverwort *Marchantia polymorpha*

Erika Bellini [a,1], Elena Bandoni [a,1], Silvia Giardini [a], Carlo Sorce [a], Carmelina Spanò [a], Stefania Bottega [a], Debora Fontanini [a], Arian Kola [b], Daniela Valensin [b], Andrea Bertolini [c], Alessandro Saba [c], Luca Paoli [a], Andrea Andreucci [a], Mingai Li [d], Claudio Varotto [d,*], Luigi Sanità di Toppi [a,**]

[a] *Department of Biology, University of Pisa, Pisa, Italy*
[b] *Department of Biotechnology, Chemistry and Pharmacy, University of Siena, Siena, Italy*
[c] *Department of Surgical, Medical and Molecular Pathology and Critical Care Medicine, University of Pisa, Pisa, Italy*
[d] *Biodiversity, Ecology and Environment Area, Research and Innovation Centre, Fondazione Edmund Mach, Trento, San Michele all'Adige, Italy*

A R T I C L E   I N F O

A B S T R A C T

Plants have evolved a set of mechanisms that control and respond to the uptake and accumulation of both essential and non-essential metals, including chelation and sequestration of these elements by thiol ligands, such as glutathione and phytochelatins. Indeed, such thiol peptides can chelate some metals, quickly form thiol-metal complexes, and segregate them in the vacuolar compartment. Reasonably, conceptually similar mechanisms can be assumed to be responsible for the transport of metal complexes– in particular thiol-cadmium complexes– across the plasma membrane, with the consequent release of this toxic metal in the extracellular environment. Such hypothesis, focusing on prevention and detoxification mechanisms, was here verified in axenically-grown gametophytes of the model liverwort *Marchantia polymorpha*, exposed to three different cadmium concentrations over five exposure times. From the data obtained, it can be deduced that the cell wall of *M. polymorpha* moderately reduced the influx of cadmium into the cells, since it was rapidly saturated by this metal. At an intracellular level, cadmium induced the activity, but not the gene expression, of the phytochelatin synthase enzyme, leading to synthesis of phytochelatins. Moreover, both glutathione and phytochelatins chelated cadmium at the cytosolic level and allowed its detoxification, possibly involving tonoplast transporters belonging to type-C ABC subfamily (*Mp7g13860* and *Mp4g11930*). Likewise, cadmium, glutathione and phytochelatins were released extracellularly, thus highlighting a possible novel role in cadmium detoxification, in a pH-dependent manner. The overall results suggest that, in *M. polymorpha*, glutathione and phytochelatins can accomplish intracellular and extracellular detoxification of cadmium.

## 1. Introduction

Cadmium (Cd) is a heavy metal widely released into the environment from natural and anthropogenic sources (Sanità di Toppi and Gabbrielli, 1999), and is deemed a major metal pollutant owing to its remarkable toxicity for all biological systems (Alloway, 2013; Ismael et al., 2019; Kubier et al., 2019). Due to their solubility, Cd and Cd-containing compounds are more mobile than other metals in environmental

matrices, possess a good bioavailability, and consequently are easily taken up by plants, where they interfere with crucial physiological processes (Clemens et al., 2013; Stanković et al., 2018).

As Cd can cause severe damage to cell structures and organelles, plants have evolved different strategies to limit its toxic effects, collectively known as "fan-shaped response" (Sanità di Toppi and Gabbrielli, 1999). This complex phenomenon includes various mechanisms that might come into play in response to Cd, both in an additive and in a synergistic way. The first line of defense of the "fan-shaped response" is aimed at preventing the Cd entry into the cell, by immobilization in the cell wall or exclusion at the plasma membrane level (Sanità di Toppi and Gabbrielli, 1999). The second line of defense consists in activating detoxification mechanisms, such as the neutralization of free Cd ions by chelation and/or sequestration in the vacuolar compartment.

In this regard, it is well known that thiol peptides, such as glutathione (GSH) and phytochelatins (PCn) (Sanità di Toppi and Gabbrielli, 1999; Clemens, 2006; Sterckeman and Thomine, 2020; and references therein), play a detoxification key role, by binding Cd and other thiophilic metals and prevent them from circulating inside the cytosol (Sanità di Toppi and Gabbrielli, 1999). GSH is a ubiquitous tripeptide of great importance to all organisms, as it performs many physiological functions, including being the precursor of PCn (Grill et al., 1985; Orwar et al., 1995; Zenk, 1996; Schröder and Collins, 2002). PCn are thiol oligopeptides able to quickly form, in the cytosol, "low molecular weight" (LMW) complexes with Cd (Vögeli-Lange and Wagner, 1990, 1996). These complexes may also acquire acid–labile sulphur ($S^{2-}$), perhaps at the tonoplast level, and form "high molecular weight" (HMW) complexes (Speiser et al., 1992), with higher affinity towards Cd ions. The vacuolar import of PCn–Cd complexes is mediated by ATP-binding cassette (ABC)-type transporters (Salt and Rauser, 1995), transmembrane proteins that utilize ATP to translocate various substrates across membranes. ABC-type proteins have a characteristic modular structure consisting in a double set of two basic elements, a hydrophobic transmembrane domain (TMD) usually made up of six membrane-spanning α-helices, and a cytosolic domain containing a nucleotide-binding domain (NBD) involved in ATP binding (Wanke and Kolukisaoglu, 2010); the two TMDs dimerize to form the substrate-binding cavity (Procko et al., 2009).

In *Arabidopsis thaliana*, the ABCC subfamily comprises 15 proteins characterized by the presence of an additional N-terminal TMD (TMD0) of unknown function (Klein et al., 2006), although it has been shown that in humans and some yeasts the C-type ABC transporters TMD0 can be involved in protein targeting (Brunetti et al., 2015). ABCC are localized in the tonoplast, and therefore they can be involved in vacuolar compartmentalization of metals and other substances. In fact, the constitutively expressed AtABCC1, AtABCC2 and AtABCC3 present in the tonoplast play a primary role in higher plants' vacuolar sequestration of PCn-Cd complexes (Park et al., 2012; Song et al., 2014).

Moreover, the *A. thaliana* G-type ABC transporter PDR8 has been involved in the extrusion of $Cd^{2+}$ or Cd conjugates across the plasma membrane of root epidermal cells (Kim et al., 2007).

Unfortunately, a high number of processes at the basis of molecular, cellular, and functional responses of bryophytes to metal(loid)s, including Cd, are poorly known, and frequently the lack of information is even total. Bryophytes are early-diverging land plants, encompassing liverworts (Marchantiophyta), mosses (Bryophyta), and hornworts (Anthocerotophyta) (Degola et al., 2022). From a phylogenetic point of view, there is nowadays mounting evidence that bryophytes are monophyletic, with hornworts sister to mosses and liverworts (Morris et al., 2018; Renzaglia et al., 2018). Bryophytes can be fundamental in studies concerning the evolution of metal detoxification systems during the transition from aquatic to terrestrial environment. Not least, such plants possess a very high surface/volume ratio, have an elevated cation exchange capacity, do not develop strong hydrophobic barriers and, consequently, are prone to free, apparently unregulated, metal absorption (Stanković et al., 2018; Bellini et al., 2021). Thus, due also to their

wide geographical distribution, bryophytes have been used as an important biological monitoring system for metal environmental pollution (Maresca et al., 2020; Bellini et al., 2021; Fasani et al., 2022).

Among bryophytes, the thalloid liverwort *Marchantia polymorpha* is an excellent model, and plays a key role in plant phylogeny (Shimamura, 2016; Bowman et al., 2017, 2022). Besides, recent advances in transformation techniques (Ishizaki et al., 2008, 2013; Kubota et al., 2013; Sugano et al., 2014) and the sequencing of the entire genome (about 280 Mb; Bowman et al., 2017) have further promoted the use of *M. polymorpha* gametophytes as a fundamental model organism in functional, molecular, and evolutionary studies of land plants. Indeed, *M. polymorpha* gametophytes offer several advantages, as they are haploid, have a short life cycle and can easily be cultivated, propagated, and crossed in axenic conditions (Kubota et al., 2013; Giardini et al., 2022). Finally, *M. polymorpha* has a high capacity for acquiring metals, and may therefore provide a valuable tool for metal biomonitoring (Sharma, 2007; Ares et al., 2018).

Thus, the purpose of this work was to mechanistically investigate some functional and molecular responses to Cd in gametophytes of *M. polymorpha*. In particular, we wanted to unravel: 1) the function of the cell wall in preventing uncontrolled intracellular Cd uptake; 2) the role of thiol peptides (GSH and PCn) as intra/extracellular Cd-detoxifying agents; 3) the contribution of some tonoplast and plasma membrane ABC-type transporters for intra/extracellular thiol peptide-Cd complex trafficking.

## 2. Materials and methods

### 2.1. Plant material, growth conditions, and experimental set-up

In v*itro* cultures of *M. polymorpha* L. subsp. *ruderalis* Bischl. and Boissel.-Dub. (Marchantiales, Marchantiophyta) female gametophytes (Cam 2–Cambridge-2 wild type, University of Cambridge, UK) were grown in Petri dishes, starting from the axenic cultivation of gemmae (from "gemmae cups"), in half-strength Murashige and Skoog (MS ½) medium (Duchefa Biochemie, Haarlem, the Netherlands), supplemented with 0.8% (w/v) sucrose (Duchefa Biochemie) and 0.7% (w/v) agar (Duchefa Biochemie). The MS ½ pH was adjusted to 5.7 with 0.1 M KOH. The culture conditions were set at 16:8 light/dark cycle, 19 ± 1 °C, and a photosynthetic photon flux density of 60 μmol m$^{-2}$ s$^{-1}$, with 60% relative humidity. After four weeks, the derived axenic gametophytes were transferred to Petri dishes for another two weeks. The six-week-old gametophytes were then moved to sterile pots filled with liquid MS ½ medium (as described above, without agar) for a further two weeks. Thereafter, the eight-week-old gametophytes (about 0.8 g FW) were individually exposed to different treatment conditions: control (MS ½ without Cd, pH 5.7) and Cd-exposed (MS ½, pH 5.7, with 10, 20, and 36 μM Cd, provided as CdSO₄ for 6, 14, 24, 72, and 120 h). After all treatments, control and Cd-exposed gametophytes were harvested and suitably prepared for the subsequent analysis. At the same time, the growth media were filtered through Minisart RC4 0.45 μm filters (Sartorius, Goettingen, Germany) and centrifuged at 20,000 × *g* (Hermle, Z 300 K, Wehingen, Germany) at 4 °C for 20 min to remove cells or cellular residues. The growth media were then aliquoted, freeze-dried and stored at − 80 °C until the time of use. Three biological replicates for each sampling time were performed for all treatments.

### 2.2. Intracellular, cell wall, and growth medium Cd content

To distinguish between total and extracellular contents of Cd an elution technique was performed (Brown and Brown, 1991; Pérez-Llamazares et al., 2010). Firstly, the gametophytes were separated from the growth medium and abundantly rinsed with deionized water to remove any residual metal ion non-specifically adhered to their surface. Then, the gametophytes were soaked by shaking them in 15 ml of a 20 mM Na₂EDTA solution for 30 min to take up fraction of the elements

bound to the cell wall (Branquinho and Brown, 1994; Sorrentino et al., 2021). The analyses of Cd in these solutions served to quantify the cell wall-bound Cd, whereas the Cd not removed from the gametophytes after this washing cycle was taken as the intracellular fraction. The total Cd content was calculated by summing the two amounts above determined. Finally, the Cd remaining in the growth medium following the metal treatments was quantified, to perform a mass balance. Prior to mineralization, the gametophytes were desiccated in oven at 60 °C for 24 h to determine their dry weight. Then, they were pulverized with a ceramic mortar and pestle and mineralized with a mixture of 3 ml of 70% $HNO_3$, 0.2 ml of 60% HF and 0.5 ml of 30% $H_2O_2$ in a microwave digestion system (Milestone Ethos 900, Milestone Srl, Italy) at 280 °C and 5.5 MPa. The concentrations of Cd were determined by ICP-MS (Perkin Elmer – Sciex, Elan 6100, Waltham, MA) and were expressed in $\mu g\ g^{-1}$ DW. Analytical quality was checked with the Standard Reference Material IAEA GBW-07604 "poplar leaves" (IAEA, 1995). The metal content remaining in the growth medium was expressed as $\mu g\ l^{-1}$ and the analytical quality was checked by the Standard Reference Material SLRS-6 "river water" (Yang et al., 2015). Recoveries were in the range 111–118%. The precision of the analysis was estimated by the relative standard deviation of 5 replicates and was < 8%. Three biological replicates were analyzed, and three technical replicates were performed for each fraction.

### 2.3. Phytochelatin synthase activity assay

*M. polymorpha* phytochelatin synthase (MpPCS) activity was assayed using recombinant MpPCS produced as described in Li et al. (2020). Firstly, purity and molecular weight of the MpPCS were characterized by 10% SDS–PAGE. Briefly, the assay was performed in 100 μl reaction buffer (200 mM HEPES-NaOH pH 8.0, 10 mM β-mercaptoethanol, 12.5 mM GSH, and 100 μM Cd provided as $CdSO_4$) containing 50 ng of recombinant MpPCS at 35 °C for 60 min, then stopped by adding 25 μl of 10% (v/v) trifluoroacetic acid and immediately analyzed by HPLC-ESI-MS-MS, set up as described in 2.4. The recombinant MpPCS activity was determined from the calculation of the amount of PCn synthesized and expressed as nmol $mg^{-1}$ MpPCS $min^{-1}$. Five biological replicates were analyzed, and three technical replicates were performed for each reaction.

### 2.4. Thiol peptide quantification in gametophytes and in growth media

Samples of control and Cd-treated gametophytes of *M. polymorpha* (100 mg FW), stored in 2 ml Eppendorf tube at − 80 °C, were extracted according to a previously published method (Bellini et al., 2020). The growth media, freeze-dried and stored at − 80 °C, were resuspended in a volume of $dH_2O$ with 200 ng $ml^{-1}$ of internal standard ($^{13}C_2$,$^{15}$N-GSH and $^{13}C_2$,$^{15}$N-PC$_2$), to concentrate the analytes 16 times. The HPLC-ESI-MS-MS analyses were all performed by an instrument layout consisting in an Agilent 1290 Infinity UHPLC (Santa Clara, CA, USA), inclusive of a thermostated autosampler, a binary pump, and column oven coupled to an AB Sciex (Concord, ON, Canada) API 4000 triple quadrupole mass spectrometer, equipped with a Turbo-V Ion spray source. A ten-port switching valve (Valco Instruments Co. Inc., Houston, TX, USA) was used as a divert valve. Chromatographic separation was performed by a reverse-phase Phenomenex (Torrance, CA, USA) Kinetex 2.6 μm XB-C18 100 Å, 100 × 3 mm HPLC column, protected by a C18 3 mm ID security guard ULTRA cartridge. Three biological replicates were analyzed, and three technical replicates were performed for each analysis. All the analyses and quantification of thiol peptides were performed following the procedures detailed in Bellini et al. (2019). System control, data acquisition and processing were carried out by an AB Sciex Analyst® version 1.6.3 software.

### 2.5. Total RNA extraction, cDNA synthesis and real-time PCR analyses

Total RNA was extracted from ground frozen tissue of *M. polymorpha* gametophytes (100 mg FW) with Spectrum Plant Total RNA Kit (Sigma-Aldrich®, Milano, Italy) following manufacturer's instructions and treated with DNaseI (Sigma-Aldrich®) for eliminating genomic DNA contamination. The integrity, quality and quantity of extracted RNA were evaluated by Qubit (Thermo Fisher Scientific, Rodano, Italy) using Qubit™ RNA IQ Assay Kit and Qubit™ RNA BR RNA Assay Kit, respectively. cDNA was synthesized from 1 μg of total RNA by High-Capacity cDNA Reverse Transcription Kit (Thermo Fisher Scientific) following manufacturer's protocol. cDNA was then diluted 10 times by adding nuclease-free water.

Amplification experiments were carried out using Eco™ Real-Time PCR System (Illumina, San Diego, CA, USA). Reactions were performed in 10 μl volumes containing 5 μl 2X EvaGreen qPCR MasterMix (Applied Biosystem Materials, Monza, Italy), 300 nM forward and reverse primers, 3 μl diluted cDNA (equivalent to 15 ng of reverse transcribed total RNA) and nuclease-free water up to 10 μl. A two-step cycle composed of denaturation at 95 °C for 15 s followed by annealing/extension at 60 °C for 60 s, was repeated 40 times and followed by a dissociation step. We analyzed the stability of three different reference genes (*M. polymorpha Actin*, *MpACT*; *Adenine Phosphoribosyl Transferase, MpAPT*; *Elogantation Factor 1, MpEF1*) under the tested conditions to choose the most stable gene to normalize expression data. Primer sequences are listed in Supplementary Table S1. To determine the amplification specificity of each primer pair prior to intensive qPCR analysis, electrophoretic analysis on agarose gel and melting curve assessment were carried out for each amplification; a single amplification band with expected size and length for each primer pair was observed on 2% agarose gels, and a single peak was detected through melting curve analysis for all amplifications. Moreover, amplification efficiencies were evaluated for all primer pairs, making sure that the efficiency was more than 90%. For evaluating if the expression of the reference genes may vary in dependence of the experimental settings, a stability analysis was performed (Saint-Marcoux et al., 2015). For this data analysis two different Excel-based algorithms have been applied: geNorm v3.510 and NormFinder v0.95311. They require relative input data, so the Cq values were converted with the formula $2^{-\Delta Ct}$ where ΔCt is the difference of each Cq value minus the lowest Cq value (highest expression level). geNorm calculates stability value (M) based on the average pairwise comparison with a stepwise exclusion of the highest M value (least stable gene). Furthermore, geNorm calculates the number of genes needed for a reliable normalization considering the pairwise variation ($V_n/V_{n+1}$) between sequential normalization factors, $NF_n$ and $NF_{n+1}$. This number is optimal when the addition of one more reference gene does not significantly contribute to the variation of the normalization factor (NFn+1) or, as suggested, the value drops below 0.15. NormFinder uses an ANOVA-based algorithm to estimate intra- and inter-group variation for a given set of experiments, providing a rank where the most stable gene is the one with lowest stability (S) value. Moreover, NormFinder provides the best gene pair combination that minimizes the expression differences among subgroups, if subgroups are set. Finally, when reference genes were selected, the $2^{-\Delta\Delta Ct}$ method was applied to calculate fold changes in all qRT-PCR analyses (Livak and Schmittgen, 2001). Three biological replicates were analyzed, and three technical replicates were performed for each reaction.

### 2.6. Photochemical efficiency

Maximum quantum yield of PSII (Fv/Fm) was measured by a chlorophyll fluorometer (Handy PEA, Hansatech Instruments, Ltd., UK) at 20 ± 1.3 °C. Gametophytes were covered with a leaf clip to adapt them to darkness for 30 min and then exposed for 1 s to 3500 μmol photons $m^{-2}$ $s^{-1}$ (650 nm peak wavelength) and chlorophyll *a* fluorescence was recorded. Nine measurements were taken for each treatment and the

fluorescence data were processed by PEA plus software (Hansatech Instruments, Pentney, King's Lynn, UK). Three biological replicates were analyzed, and three technical replicates were performed up to nine measurements for each sample.

## 2.7. Electrolyte leakage assay

Membrane injury was estimated by electrolyte leakage as in Balestri et al. (2014) with minor modifications. After a thorough washing, squared submarginal portions of gametophyte (1 cm$^2$) were incubated in deionized water, evacuated for 30 min, and allowed gently stirring for 22 h at 4 °C. The conductivity of the aqueous solution was measured at 25 °C with a Jenway 4310 Conductivity Meter (Cole-Parmer, Stone, UK). After boiling the test tubes in a water bath for 30 min, conductivity was detected at 25 °C. The percentage of membrane damage was calculated by the formula:

$$(C1 - Cw)/(C2 - Cw) \times 100$$

where C1 is the electro-conductance value of samples at the first measurement, C2 is the electro-conductance value after boiling, and Cw is the electro-conductance value of deionized water. Data were normalized

by setting the values of the control samples equal to 1. Five biological replicates were analyzed for each condition.

## 2.8. NMR measurements of GSH-Cd binding

NMR analyses were performed with 600 MHz Bruker Avance spectrometer (Bruker, Ettlingen, Germany), equipped with a Sensitive Enhancement Improvement (SEI) probe. NMR spectra were processed and analyzed by using the TopSpin 3.6.4 software. Suppression of residual water signal was obtained by excitation sculpting pulse program, applying a selective 2 msec long square pulse on water (Hwang and Shaka, 1998). All the experiments were collected at 298 K. Pure GSH samples (Sigma-Aldrich®) were dissolved in water with 10% of D$_2$O, and the pH was adjusted at 3.5 and 6.0 by adding small volumes of HCl or NaOH. Two different GSH concentrations were used: 1.0 and 10.0 mM, for $^1$H and $^{13}$C NMR, respectively. Proton and carbon resonance assignment was achieved by the combined analysis of $^1$H–$^1$H TOCSY and $^1$H–$^{13}$C HMBC 2D spectra. The additions of Cd$^{2+}$ to GSH samples were obtained by using CdCl$_2$ stock solutions. The pH of all samples was checked before and after each Cd addition. Chemical shifts were referred to TMSP-d$_4$ (3-(trimethylsilyl)propionic-2,2,3,3-d$_4$ acid
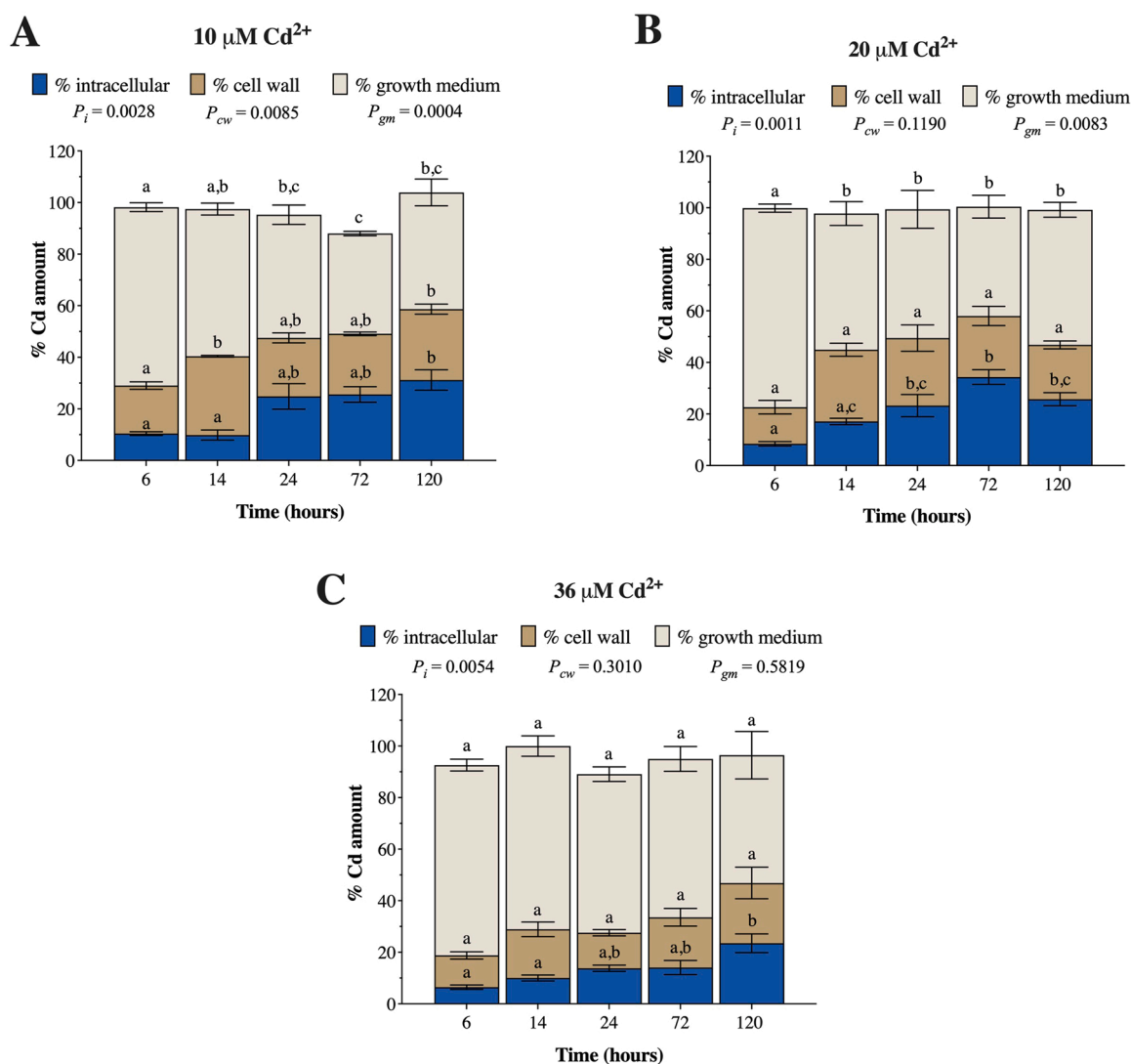


**Fig. 1.** Percentage of total Cd detected in symplasm (blue bars), cell wall (brown bars) and growth medium (pale brown bars) of *M. polymorpha* gametophytes treated with (A) 10 μM Cd$^{2+}$, (B) 20 μM Cd$^{2+}$, and (C) 36 μM Cd$^{2+}$ for 6, 14, 24, 72, and 120 h. Values are mean ± SE, n = 3 (one-way ANOVA, followed by Tukey's *post-hoc* test). Different letters indicate significant differences at $P < 0.05$ within the same compartment(s) at different exposure times. $P_i = P$ for intracellular Cd; $P_{cw} = P$ for cell wall-bound Cd; $P_{gm} = P$ for Cd detected in the growth medium.

sodium salt), used as NMR internal standard.

### 2.9. Statistical analyses

Data were analyzed by means of the Graph-Pad Prism 8.2.1 statistical program (GraphPad Software Inc., San Diego, CA, USA). Data were reported as the mean ± SE (standard error). The threshold of statistical significance was set at $P < 0.05$, unless otherwise specified. One-way and two-way analysis of variance (ANOVA), followed by Tukey's multiple comparison *post-hoc* test, was performed. The details of each test applied to the results are given in the figure captions.

## 3. Results

### 3.1. Fast cell wall saturation partly overcomes its ability to delay Cd intracellular absorption

ICP-MS analyses of Cd distribution in *M. polymorpha* gametophytes showed that the cell wall acted as a barrier towards the metal intracellular absorption, but it was saturated within the first few hs of treatment, for all the three concentrations of Cd employed (10, 20, and 36 μM). The Cd immobilized by the cell wall remained constant in all treatments at values of around 20% of the total amount supplied (Fig. 1). On the other hand, Cd entered the symplasm in all treatments, with a significant increase over time for all concentrations supplied (Fig. 1). Accordingly, within each Cd concentration provided, the metal quantified in the growth medium decreased over time (Fig. 1), in some cases at least as a trend. Indeed, at the highest concentration of 36 μM Cd, the metal found in the growth medium was more abundant compared to the other two metal concentrations supplied, apparently at the expense of the intracellular and cell wall-bound Cd (Fig. 1).

### 3.2. The presence of intracellular Cd stimulates PCS activity but not its gene expression

To assess the responsiveness of gametophytes' *MpPCS* to Cd exposure, qPCR analyses were performed over time under the highest Cd concentration tested, using both *MpACT* and *MpEF1* as reference housekeeping genes. The best combination of the two genes was selected after stability analysis (results in Table S2). The expression analysis showed that *MpPCS* was constitutively transcribed, also in untreated gametophytes (Fig. S1). A slight but non-significant increase in transcript levels was observed after 6 h of treatment, showing a substantial absence of modulation at the transcriptional level (Fig. S1).

Furthermore, the *in vitro* activity assay of MpPCS recombinant protein (57 kDa; Fig. 2A) was performed, to confirm the Cd-promoted activation of the enzyme (Fig. 2B, right column) in comparison with Cd-untreated samples (Fig. 2B, left column). The results confirmed that the enzyme was markedly activated by Cd (Fig. 2B, right column).

### 3.3. Cd stimulates thiol peptide production without affecting the gene expression of two putative vacuolar transporters

With regard to thiol peptide production *in vivo*, low and constant

levels of GSH were detected over time in control gametophytes (Fig. 3A), whereas significantly higher GSH concentrations than controls were detected in Cd-exposed samples (Fig. 3A). Likewise, under Cd treatments, a significant increase in the production of PCn (PC$_2$, PC$_3$, PC$_4$) was recorded, reaching approx. constant levels after the different exposure times, with slight differences depending on Cd concentrations (Fig. 3B, C, D). As in the *in vitro* assay (Fig. 2B, left column), also *in vivo* PC$_2$ resulted to be the most abundant PCn produced in response to Cd; PC$_2$ was detected in Cd-untreated gametophytes, as well (Fig. 3B). By contrast, PC$_3$ and PC$_4$ were synthesized only in response to Cd-treatments, and their levels increased over time, reaching a plateau after 24 h (PC$_3$) and 72 h (PC$_4$) (Fig. 3C, D).

Moreover, the results obtained from the alignment of the cDNA sequences of the two *A. thaliana* tonoplast transporters (AtABCC1 and AtABCC2) showed that both provide the same sequence in *M. polymorpha* as the best alignment (accession number: OAE21808.1, corresponding to *Mp7g13860*), with very similar identity, around 60%. The amino acid sequence alignment between AtABCC1, AtABCC2 and the putative protein encoded by *Mp7g13860* are shown in Fig. S2. In addition, the sequence with the highest identity percentage and the best query coverage (accession number: BBN08481.1, corresponding to *Mp4g11930*) was selected based on the alignment with the sequence of AtABCC3 of *A. thaliana*. The amino acid sequence alignment between AtABCC3 and the putative protein encoded by *Mp4g11930* are shown in Fig. S3.

The relative expression levels of the two genes identified in *M. polymorpha* genome were evaluated by real-time PCR. The results showed an overall quite similar response of the two transporters to Cd supply at the highest concentrations (Fig. S4). In the case of *Mp7g13860*, a significant decrease in the expression level was observed only after 14 h of treatments with highest Cd concentration, whereas at the other exposure times no differences were found between controls and Cd-treated samples (Fig. S4A). Likewise, *Mp4g11930* expression levels did not vary significantly compared to the controls (Fig. S4B).

### 3.4. GSH and PCn can be released extracellularly

The quali-quantitative analysis of thiol peptides by HPLC-ESI-MS-MS was carried out also in growth media, and revealed the extracellular presence of both GSH and PCn, up to PC$_4$ (Fig. 4). In general, the highest concentrations of such thiol peptides were recorded at the highest Cd concentration and at longer times (Fig. 4), although their detection was possible, on the whole, already after the first hs of treatment at low Cd concentrations (Fig. 4C, D). Moreover, as found in the intracellular analysis, GSH and PC$_2$ were detected also in the growth medium of Cd-untreated samples (Fig. 4A, B) (see 3.3).

A comparison of the HPLC-ESI-MS-MS results between the growth media and the gametophytes showed a considerable difference in the intracellular and extracellular concentrations of GSH and PCn (Fig. 5). The extracellular GSH content was about an order of magnitude lower than the intracellular one (Fig. 5A, C), whereas the extracellular PCn content was nearly two orders of magnitude lower (Fig. 5B, D). Indeed, the extracellular thiol peptide concentrations gradually increased with rises in Cd concentrations and exposure times, albeit with a different
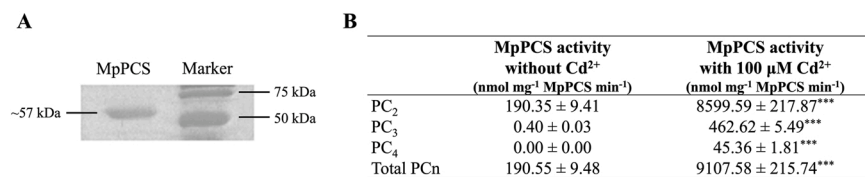
**A**

MpPCS　　Marker

~57 kDa —

— 75 kDa
— 50 kDa

**B**

| | MpPCS activity without Cd$^{2+}$ (nmol mg$^{-1}$ MpPCS min$^{-1}$) | MpPCS activity with 100 μM Cd$^{2+}$ (nmol mg$^{-1}$ MpPCS min$^{-1}$) |
|---|---|---|
| PC$_2$ | 190.35 ± 9.41 | 8599.59 ± 217.87*** |
| PC$_3$ | 0.40 ± 0.03 | 462.62 ± 5.49*** |
| PC$_4$ | 0.00 ± 0.00 | 45.36 ± 1.81*** |
| Total PCn | 190.55 ± 9.48 | 9107.58 ± 215.74*** |

**Fig. 2.** (A) Recombinant MpPCS protein purified from *E. coli* and electrophoresed in 12.5% SDS-PAGE. The left-hand lane is the recombinant MpPCS and the right-hand one is the protein size marker (Precision Plus Protein™ Dual color Standards, BioRad, Italy); two different sizes (75 and 50 kDa) are shown for the corresponding bands in the marker. (B) *In vitro* activity of recombinant protein MpPCS upon activation with 100 μM Cd$^{2+}$ (right column) or 0 μM Cd$^{2+}$ (Cd-unexposed samples (left column) for 60 min at 35 °C in the proper reaction mixture. PCS activity is expressed in nmol PCn mg$^{-1}$ MpPCS min$^{-1}$. Values are mean ± SE, n = 5 (unpaired *t test* between PCn production without Cd$^{2+}$ and with 100 μM Cd$^{2+}$; * $P \leq 0.05$; ** $P \leq 0.01$; *** $P \leq 0.001$).
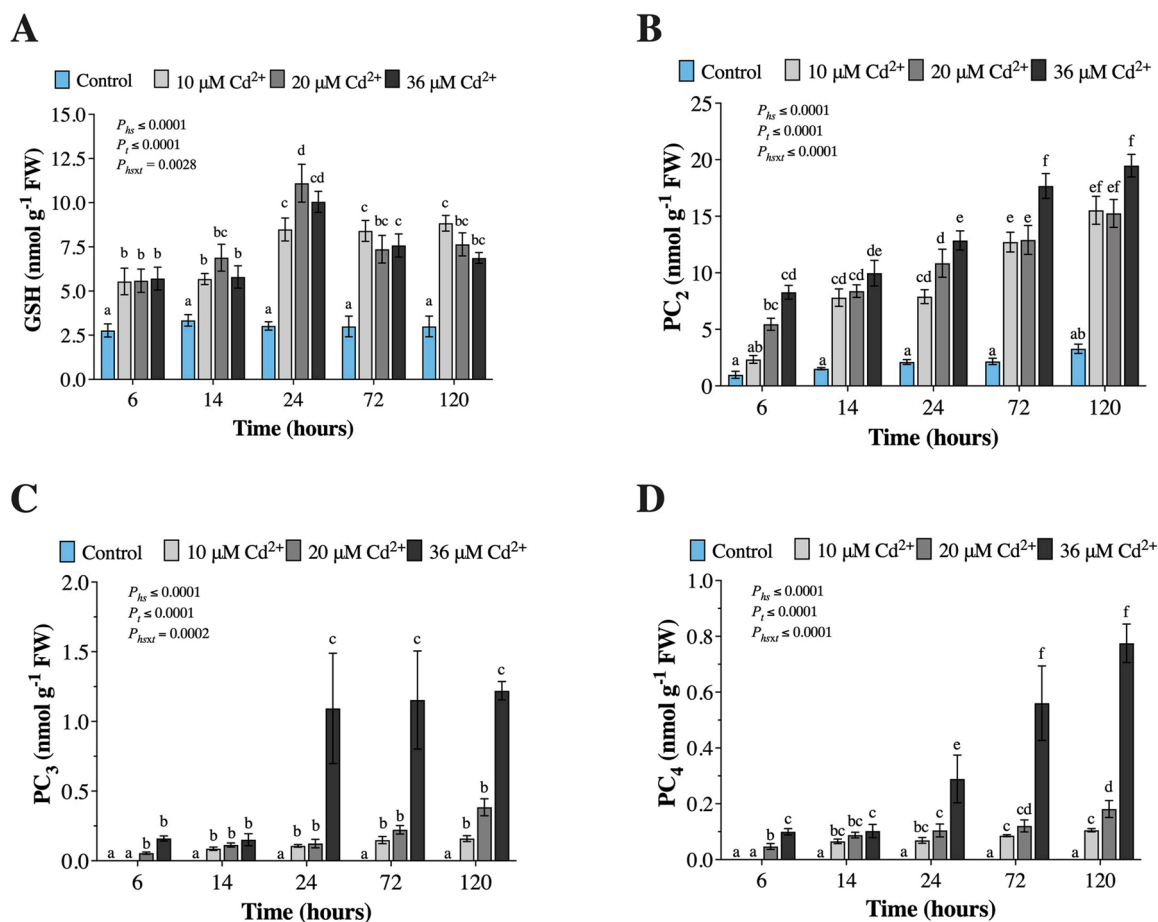
**A**



**B**



**C**



**D**



**Fig. 3.** (A) Glutathione (GSH), (B) phytochelatin 2 ($PC_2$), (C) phytochelatin 3 ($PC_3$), and (D) phytochelatin 4 ($PC_4$) concentrations (nmol g$^{-1}$ FW) in *M. polymorpha* gametophytes, following exposure for 6, 14, 24, 72, and 120 h to 0 (control), 10, 20, and 36 µM Cd$^{2+}$. Values are mean ± SE, n = 3 (two -way ANOVA, followed by Tukey's *post-hoc* test). Different letters indicate significant differences at $P < 0.05$ between different concentrations and exposure times. $P_{hs} = P$ for exposure time effects; $P_t = P$ for treatment effects; $P_{hsxt} = P$ for the interaction time x treatment effects.

trend from that observed intracellularly (Figs. 3–5).

### 3.5. Cd does not compromise photosynthetic efficiency and membrane status

To evaluate the induction of stress by Cd treatments, whole-plant photochemical efficiency and electrolyte leakage were measured. The results of fluorescence analysis showed no significant Cd-induced differences in maximum PSII quantum yield (Fv/Fm), confirming that the chosen treatments did not compromise photosynthetic efficiency (Fig. S5A). Likewise, the membrane status assessed by the electrolyte leakage conductivity showed no Cd-induced damage in gametophytes other than a slight increase in membrane permeability at a 120 h-treatment (Fig. S5B).

### 3.6. GSH ability to form complexes with Cd is pH-dependent

NMR analysis was carried out to investigate in which way thiol-Cd complexes were formed, in order to understand whether or not they can be potentially assembled in the extracellular environment. In particular, we focused our attention on assessing Cd-GSH binding and conformation at two different pH values, 6.0 and 3.5, which were chosen according to the internal and external pH values experienced by the gametophytes upon exposure to Cd$^{2+}$ (Giardini et al., 2022).

At pH 6.0, Cd$^{2+}$ addition caused selective and significant $^1$H and $^{13}$C chemical shift variations on GSH nuclei. As shown in Fig. 6, the most affected protons are H$_N$ of Cys and Gly, H$_\alpha$ of Gly and H$_\beta$ of Cys, being the

latter the most shifted one.

As previously detected on $^1$H nuclei, the $^{13}$C resonances of GSH were largely perturbed upon metal addition. The Cd-induced variations were in fact mainly detected as strong line broadening of the NMR signals rather than changes on the chemical shifts (Fig. S6). The obtained results showed that the largest effects were still observed on Cys resonances (CO, C$_\alpha$ and C$_\beta$). Moreover, Cd-GSH interaction at pH 6.0 resulted in the disappearance of CO signal of γGlu, as indicated in Fig. S6A.

The metal induced changes of NMR signals strongly support the Cd$^{2+}$ binding to GSH. Indeed, the formed metal complex leads to a substantial electron density change in the area around the metal center, explaining the effects recorded on $^1$H and $^{13}$C nuclei (Fig. 6, Fig. S6). Such variations are graphically represented as colored circles in the GSH molecular structure, in order to identify the Cd binding region (Fig. 7A). By considering that the larger the NMR effects are, the closer the nuclei to the metal coordination sphere are, the two Cys thiol groups were identified as the metal donor atoms (Fig. 7B). Such findings are consistent with the formation of Cd(GSH)$_2$ *bis*-complex with the metal ion, coordinated to two Cys sulfur atoms, in agreement with previous data (Delalande et al., 2010).

Since metal binding is markedly dependent on pH values, a similar NMR analysis was performed also at pH 3.5, for evaluating the Cd binding abilities and characterizing the formed metal complexes at this pH value. Upon Cd$^{2+}$ addition, no effects were observed on $^1$H NMR signals (data not shown). On the other hand, slight chemical shift variations were detected on $^{13}$C nuclei of the carboxylate groups of γGlu and Gly (Fig. S7). These two signals, overlapping in a unique NMR resonance
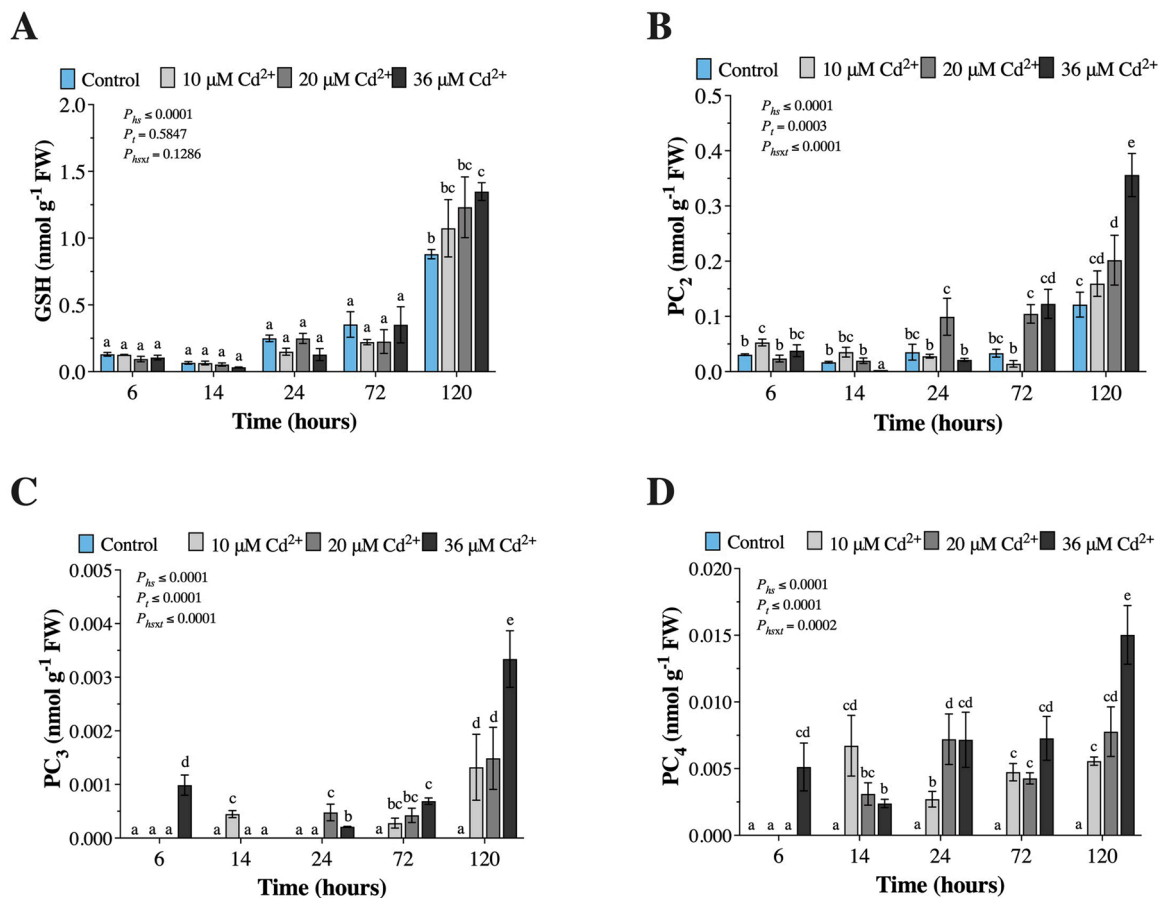
**A**



**B**



**C**



**D**



**Fig. 4.** (A) Glutathione (GSH), (B) phytochelatin 2 ($PC_2$), (C) phytochelatin 3 ($PC_3$), and (D) phytochelatin 4 ($PC_4$) concentrations (nmol $g^{-1}$ FW) determined in the growth medium, following exposure for 6, 14, 24, 72, and 120 h to 0 (control), 10, 20, and 36 µM $Cd^{2+}$. Values are mean ± SE, n = 3 (two-way ANOVA, followed by Tukey's *post-hoc* test). Different letters indicate significant differences at $P < 0.05$ between different concentrations and exposure times. $P_{hs} = P$ for exposure time effects; $P_t = P$ for treatment effects; $P_{hsxt} = P$ for the interaction time x treatment effects.

in the free ligand, exhibited two clear and separated resonances in the metal GSH complex. The effects are represented in Fig. 7C, D, and support $Cd^{2+}$ binding to the acidic carboxylate groups at pH 3.5.

The obtained findings indicate that GSH is able to interact with $Cd^{2+}$ both at pH 6.0 and at pH 3.5, by forming two different metal complexes, being the $Cd^{2+}$ coordination sphere and binding affinity strongly dependent on pH. The chemical shift variations are more evident at pH 6.0 than at pH 3.5, suggesting a tighter binding affinity at higher pH. In addition, the two Cys thiolate groups coordinated to $Cd^{2+}$ at pH 6.0 are substituted by carboxylate groups at lower pH values (Fig. 7C, D).

*3.7. Expression analysis of a M. polymorpha homolog of the AtPDR8 transporter indicates a marked decrease of transcription levels*

*A. thaliana* PDR8, a G-type ABC transporter, has been implicated in the extrusion of $Cd^{2+}$ or Cd conjugates across the plasma membrane (Kim et al., 2007). The *M. polymorpha* closest homolog of AtPDR8, according to blastx searches, is encoded by *Mp2g21800* (Genbank accession number: BBN03227.1). The amino acid sequence alignment between the putative protein encoded by *Mp2g21800* and AtPDR8 is shown in Fig. S8.

To test whether the transcription levels of *Mp2g21800* are responsive to $Cd^{2+}$, expression of the gene in presence of 36 µM $Cd^{2+}$ was evaluated by real-time PCR. Results showed a marked decrease of gene transcription levels from 14 h onwards (Fig. S9).

## 4. Discussion

The "fan-shaped response" is a general model that well describes the complex network of mechanisms involved in the response to Cd in higher plants (Sanità di Toppi and Gabbrielli, 1999). However, such mechanisms are largely unknown for bryophytes, despite many species of mosses, liverworts, *etc.*, can represent fundamental tools in bio-monitoring techniques, due to their elevated capacity to absorb metal (loid)s (González and Pokrovsky, 2014; Ares et al., 2018; Bellini et al., 2021; and references therein). It has been known, for example, that the high metal accumulation capacity in mosses is largely due to the sorption and retention given by their cell walls (Ross, 1990), which are particularly rich in metal-binding homogalacturonans and other poly-saccharides (Stanković et al., 2018; Tyler, 1990; Pfeifer et al., 2022). The binding of metal ions to the cell wall reduces the amounts of metals entering the symplast, and thus constitutes an important avoidance mechanism, at least for mosses (Basile et al., 2009; Spagnuolo et al., 2011; Basile et al., 2012; Lazo et al., 2013; Stanković et al., 2018).

Also in the liverwort *M. polymorpha*, subject of this study, the cell wall plays a role in slowing down the Cd entry into the cytosol, but such an avoidance mechanism is effective only in the very early phases of exposure to this toxic metal, since already after 6 hs the binding capacity of the cell wall reaches an apparent saturation. Thus, a limited availability of metal binding sites in *M. polymorpha* cell walls can be evidenced, at least in the experimental conditions tested. According to Parrotta et al. (2015) and Pfeifer et al. (2022), the chemical composition of the cell wall amongst bryophytes can vary significantly, and this can obviously affect the ability of this structure to retain heavy metals. For
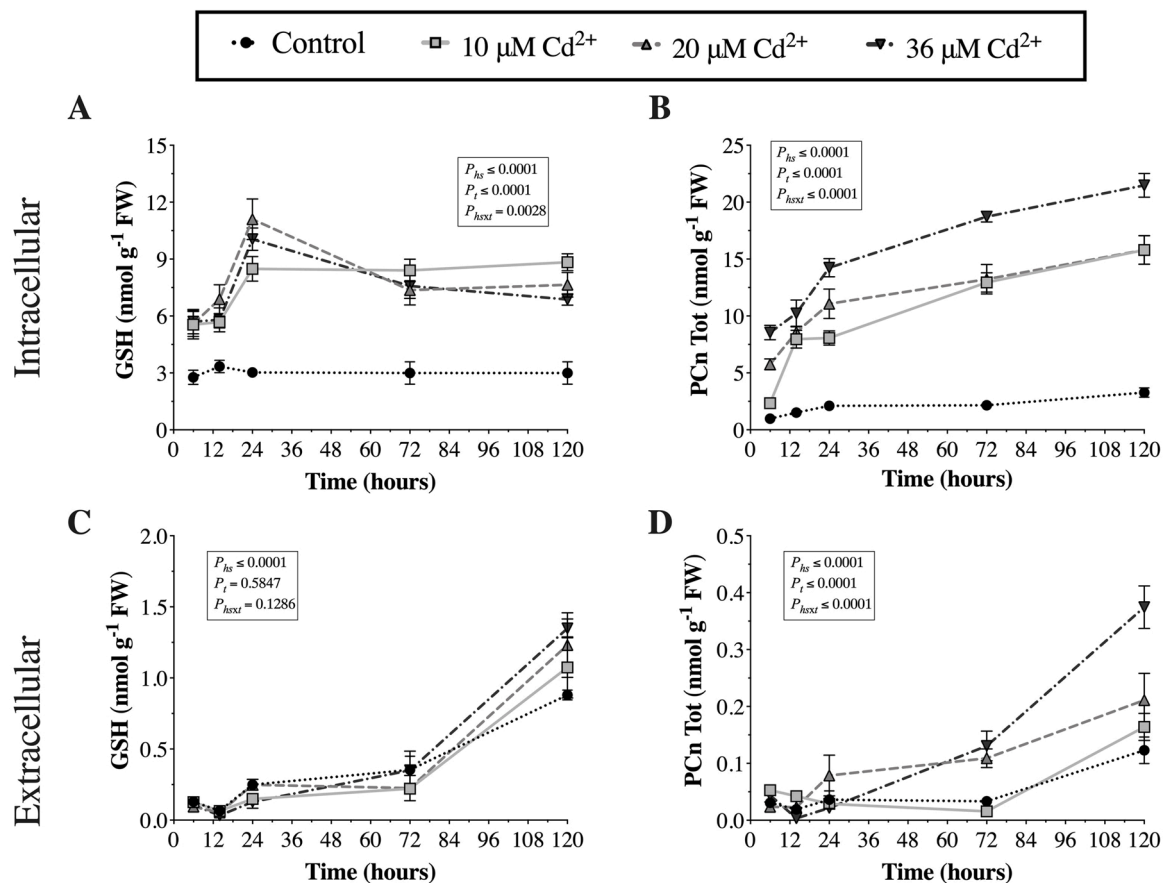
**Fig. 5.** Time course of intracellular (A) GSH and (B) PCn content (nmol g$^{-1}$ FW) in *M. polymorpha* gametophytes, following exposure for 6, 14, 24, 72, and 120 h to 0 (control), 10, 20, and 36 μM Cd$^{2+}$. Time course of (C) GSH and (D) PCn (nmol g$^{-1}$ FW) present in the medium where the gametophytes were grown, at the same Cd$^{2+}$ concentrations and exposure times as above. Values are mean ± SE, n = 3 (two-way ANOVA). $P_{hs}$ = P for exposure time effects; $P_t$ = P for treatment effects; $P_{hsxt}$ = P for the interaction time x treatment effects.
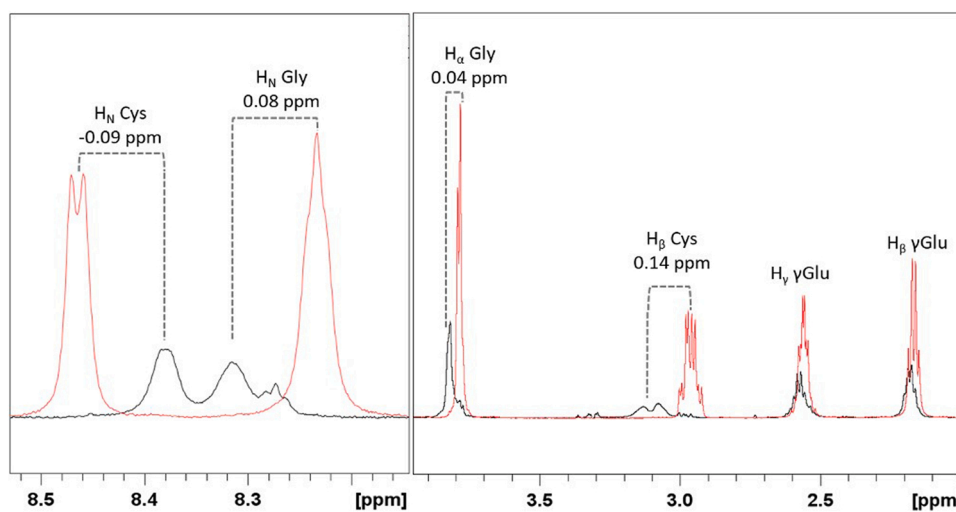


**Fig. 6.** Selected regions of $^1$H NMR spectrum of GSH 1.0 mM, pH = 6.0 and T = 298 K, in the absence (red trace) and presence of 0.5 Cd$^{2+}$ eqs. The chemical shift variations (Δδ) of Cys and Gly protons are shown.

example, the liverwort *Dumortiera hirsuta* – a different species from *Marchantia polymorpha*, but not too phylogenetically distant from the latter – showed that the ratio between the overall extracellular and intracellular Cd varied in the range of 10–20 times (Mautsoe and Beckett, 1996), while in our case the same ratio varied between about 5 and 10 times, but in the presence of much lower concentrations of Cd,

employment of another chelating agent and different species/experimental systems. Moreover, Mautsoe and Beckett (1996) did not distinguish between cell wall Cd values and those found in the growth medium, since their cultures were not *in vitro* and axenic-grown, like ours. All this stated, we believe that the Cd retained by the cell wall should be conceptually discerned from that found in the growth
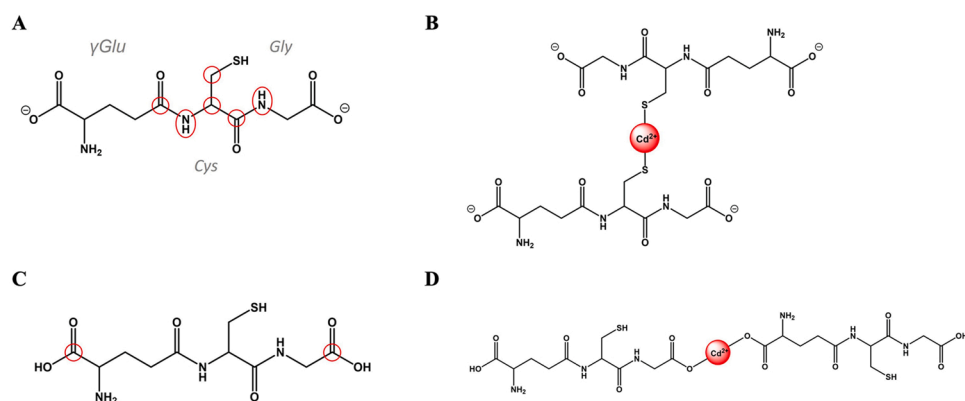
**Fig. 7.** (A) Molecular structure of GSH. Circled atoms correspond to nuclei exhibiting the largest NMR changes at pH 6.0. (B) Model of Cd $(GSH)_2$ complex at pH 6.0, showing the metal binding to thiol groups of two GSH molecules (the represented metal coordination sphere does not take into account the metal geometry). (C) Molecular structure of GSH. Circled atoms correspond to nuclei exhibiting the largest NMR changes at pH 3.5. (D) Model of Cd$(GSH)_2$ complex at pH 3.5, showing the metal binding to carboxylate groups of two GSH molecules (the represented metal coordination sphere does not take into account the metal geometry).

medium, as the latter could be specifically released by the symplasm, as hypothesized in our work. We can therefore get evidence that, under the experimental conditions described here, the amount of Cd retained by the cell wall of *M. polymorpha* gametophytes is comparable to that found intracellularly, and that in this liverwort the cell wall does not seem to play a fundamental role in the defence against Cd toxicity.

Passed the cell wall barrier, the entry of bivalent metal cations into the symplasm of higher plants is controlled by common regulators and transporters, such as IRT1 (*ZIP* gene family) and Nramp, which can transport several metals including Cd (Pence et al., 2000; Sterckeman and Thomine, 2020). Thus, it is likely that similar mechanisms may operate also in *M. polymorpha*, where the intracellular translocation of Cu, Zn, and Cd has already been reported (Ares et al., 2018). In parallel to the symplasmic increase of Cd, several lines of evidence indicate that the activation of detoxifying pathways is related to metal chelation and vacuolar sequestration. In this respect, intracellular thiol peptides seem to play a crucial role in *M. polymorpha* gametophytes. The present results broaden our previous observations (Bellini et al., 2020; Li et al., 2020; 2022): Cd exposure not only activates the constitutively expressed enzyme MpPCS, leading to a significant increase in total PCn produced, but also enhances the GSH levels. Thus, overall, the synthesis of GSH exceeds its consumption for PCn production, confirming its involvement in other detoxifying metabolic pathways (Foyer and Noctor, 2001; Schafer and Buettner, 2001). Among the PCn, $PC_2$ was produced in the shortest time and at highest levels, but also $PC_3$ and $PC_4$ were synthesized, especially at the highest Cd concentration. The latter were produced mainly after 24 h of Cd treatment, since PCn with higher degrees of polymerization are more efficient chelators when the Cd stress is more intense, due to the greater number of thiol groups in their structure (Kneer and Zenk, 1997). In a previous work regarding *M. polymorpha*, with GUS reporter lines driven by the *MpPCS* promoter, semi-quantitative RT-PCR analyses evidenced the constitutive transcription of the gene in the absence of Cd, as well as minor variations in its transcription in the first hs of metal treatment (Li et al., 2020). In the present study, a more detailed gene expression analysis confirmed the constitutive transcription of *MpPCS*, as also observed in other plants (Meyer et al., 2011).

It is known that PCn, once having complexed Cd, can be compartmentalized in the vacuole through the action of tonoplast C-type ABC transporters (Song et al., 2010; Brunetti et al., 2015). In the present work, the two closest *M. polymorpha* homologs of *A. thaliana* AtABC-C1/AtABCC2 and AtABCC3, *Mp7g13860* and *Mp4g11930*, respectively, were shown to be constitutively expressed. Indeed, under Cd stress, no Cd-mediated modulation of the expression of these transporters was evidenced - except for a decrease in *Mp7g13860* expression level only after 14 h of treatment with highest Cd concentration -, unlike what was observed in *A. thaliana* (Park et al., 2012; Brunetti et al., 2015). Thus, it may be postulated that the constitutive level of expression of *Mp7g13860* and *Mp4g11930* might be sufficient for playing their role(s).

Indeed, not all genes that have important functional role(s) in response to stressful conditions should necessarily undergo transcriptional changes to play such role(s). In fact, the presence of multiple paralogs with analogous function(s), or higher constitutive levels of expression and/or enzyme activity, may render the transcriptional changes of transporters unnecessary.

Furthermore, since the plasma membrane transporters involved in the extrusion of free Cd ions or Cd conjugates have not yet been identified in bryophytes, we also chose to analyze the *Mp2g21800* gene, which is the closest homologue to the *A. thaliana* AtPDR8. This protein is part of the G-type ABC transporters family; in other plants, such as *A. thaliana* and *Oryza sativa*, is known to be localized in the plasma membrane and to be involved in translocation of Cd across the membrane (Kim et al., 2007; Fu et al., 2019). Our results showed that *Mp2g21800* was constitutively expressed, but its expression levels decreased in the presence Cd, contrary to what has been reported in the literature for PDR genes in higher plants (Kim et al., 2007; Fu et al., 2019). Indeed, the Mp2g21800 protein may be stabilized by Cd and, consequently, a higher expression might be unnecessary. Moreover, at least in bryophytes – and particularly in the liverwort *M. polymorpha* – different transporter(s) can be involved in metal trafficking through the plasma membrane. Because plant transporters are often promiscuous in terms of substrates, and a few amino acid substitutions can be sufficient to change their specificity towards metal(loid) ions, the exact role of each transporter has to be experimentally determined specifically *in planta* (Martinoia, 2018). According to Kobae et al. (2006), the actual substrate is unknown for most plant PDRs, with the exceptions of SpTUR2 and NpPDR1. In other words, many publications on metal transporters reveal that, in different plants, their homologs often exhibit different specificities (Martinoia, 2018; Zeng et al., 2020).

Finally, in the present work a new hypothesis on the possible role of thiol peptides - not only as intracellular but also as extracellular detoxifying agents - has been explored. Our evidence is that thiol peptides (GSH and PCn) are released by *M. polymorpha* gametophytes as thiol-Cd complexes, and not only as free thiols: this is supported by the NMR analyses on the pH-dependent ability to form complexes with Cd. The GSH was chosen as the model thiol peptide for NMR, as it resulted to be the most abundant in the growth medium. Extensive investigations of GSH-$Cd^{2+}$ complexes were previously carried out by some research groups, and showed that the coordination chemistry of both GSH and PCn is highly dynamic (Połeć-Pawlak et al., 2007; Delalande et al., 2010; Uraguchi et al., 2021). Our data evidenced that a pH of 6.0 (approximately corresponding to that of the cytosol) was suitable for the formation of stable thiol-Cd complexes, whereas a pH of about 3.5, such as that measured in the growth media (Giardini et al., 2022), did not promote the formation of stable complexes. Therefore, a possible novel mechanistic model, depicted in Fig. 8, is proposed.
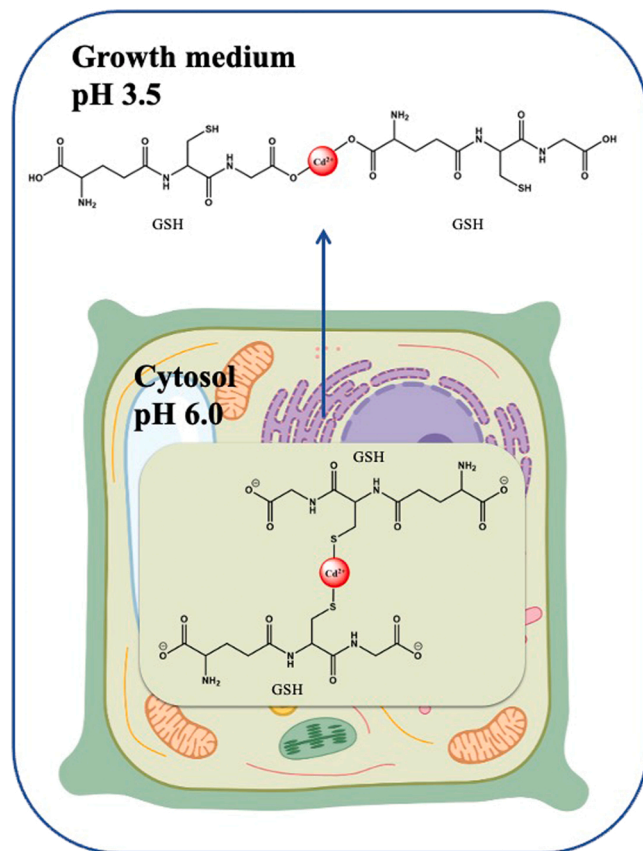
**Fig. 8.** Mechanistic model proposed about the pH-dependent formation and movement of GSH-Cd complexes in *M. polymorpha*, based on NMR results (NB: a conceptually similar model might also be extended to PCn): Cd enters the cytosol where the GSH-Cd complexes are formed *via* the thiol groups of two GSH molecules. The complexes are in part transported into the vacuole and in part released outside the cells, where the metal is bound to the carboxylate groups of two GSH molecules, due to the extracellular acidic pH. After that, the complexes are quickly broken down and the free Cd ions and thiols are released. This coordinated response appears to be efficient in contributing to prevent Cd damages, as suggested by the unaffected Fv/Fm ratio and by the overall levels of membrane leakage.

## 5. Conclusions

From the set of data presented in this work, it appears that the liverwort *M. polymorpha* possesses a cell wall only partially able to counteract Cd intracellular penetration, due to its early saturation. Indeed, the presence of intracellular Cd stimulates PCS activity, and the subsequent metal-induced production of PCn allows the intracellular Cd detoxification. However, GSH and PCn can also be released extracellularly, and this might be considered a new concurrent system of Cd detoxification, too. Indeed, GSH ability to form complexes with Cd appears to be pH-dependent.

## Funding

## CRediT authorship contribution statement

**Erika Bellini**: Methodology, Data curation, Writing – original draft preparation. **Elena Bandoni**: Methodology, Data curation, Writing – original draft preparation. **Silvia Giardini**: Methodology. **Carlo Sorce**: Methodology, Data curation, Writing – original draft preparation. **Carmelina Spanò**: Methodology, Data curation. **Stefania Bottega**: Methodology. **Debora Fontanini**: Methodology. **Arian Kola**: Methodology. **Daniela Valensin**: Conceptualization, Data curation, Writing – original draft preparation. **Andrea Bertolini**: Methodology. **Alessandro Saba**: Methodology. **Luca Paoli**: Methodology. **Andrea Andreucci**: Methodology. **Mingai Li**: Methodology, Data curation. **Claudio Varotto**: Conceptualization, Writing – original draft preparation, Supervision. **Luigi Sanità di Toppi**: Conceptualization, Data curation, Writing – original draft preparation, Supervision, Project administration, Funding acquisition, Responsibility for the integrity of the work as a whole.

## Declaration of Competing Interest

The authors declare that they have no known competing financial interests or personal relationships that could have appeared to influence the work reported in this paper.

## Data availability

Data will be made available on request.

## Appendix A. Supporting information

Supplementary data associated with this article can be found in the online version at doi:10.1016/j.envexpbot.2023.105303.

## References

Alloway, B.J., 2013. Heavy Metals in Soils. Springer,, Netherlands. https://doi.org/10.1007/978-94-007-4470-7.

Ares, Á., Itouga, M., Kato, Y., Sakakibara, H., 2018. Differential metal tolerance and accumulation patterns of Cd, Cu, Pb and Zn in the liverwort *Marchantia polymorpha* L. Bull. Environ. Contam. Toxicol.. 100 (3), 444–450. https://doi.org/10.1007/s00128-017-2241-0.

Balestri, M., Bottega, S., Spanò, C., 2014. Response of *Pteris vittata* to different cadmium treatments. Acta Physiol. Plant. 36, 767–775. https://doi.org/10.1007/s11738-013-1454-z.

Basile, A., Sorbo, S., Aprile, G., Conte, B., Castaldo Cobianchi, R., Pisani, T., Loppi, S., 2009. Heavy metal deposition in the Italian "triangle of death" determined with the moss *Scorpiurum circinatum*. Environ. Pollut. 157 (8–9), 2255–2260. https://doi.org/10.1016/J.ENVPOL.2009.04.001.

Basile, A., Sorbo, S., Pisani, T., Paoli, L., Munzi, S., Loppi, S., 2012. Bioaccumulation and ultrastructural effects of Cd, Cu, Pb and Zn in the moss *Scorpiurum circinatum* (Brid.) Fleisch. and Loeske. Environ. Pollut. 166, 208–211. https://doi.org/10.1016/j.envpol.2012.03.018.

Bellini, E., Borsò, M., Betti, C., Bruno, L., Andreucci, A., Ruffini Castiglione, M., Saba, A., Sanità di Toppi, L., 2019. Characterization and quantification of thiol-peptides in *Arabidopsis thaliana* using combined dilution and high sensitivity HPLC-ESI-MS-MS. Phytochemistry 164, 215–222. https://doi.org/10.1016/J.PHYTOCHEM.2019.05.007.

Bellini, E., Varotto, C., Borsò, M., Rugnini, L., Bruno, L., Sanità di Toppi, L., 2020. Eukaryotic and prokaryotic phytochelatin synthases differ less in functional terms than previously thought: A comparative analysis of *Marchantia polymorpha* and *Geitlerinema* sp. PCC 7407. Plants 9 (7), 1–12. https://doi.org/10.3390/plants9070914.

Bellini, E., Betti, C., Sanità di Toppi, L., 2021. Responses to cadmium in early-diverging streptophytes (charophytes and bryophytes): Current views and potential applications. Plants 10 (4), 770. https://doi.org/10.3390/plants10040770.

Bowman, J.L., Kohchi, T., Yamato, K.T., Jenkins, J., Shu, S., Ishizaki, K., Yamaoka, S., Nishihama, R., Nakamura, Y., Berger, F., Adam, C., Aki, S.S., Althoff, F., Araki, T., Arteaga-Vazquez, M.A., Balasubrmanian, S., Barry, K., Bauer, D., Boehm, C.R., Schmutz, J., 2017. Insights into land plant evolution garnered from the *Marchantia polymorpha* genome. e15 Cell 171 (2), 287–304. https://doi.org/10.1016/j.cell.2017.09.030.

Bowman, J.L., Arteaga-Vazquez, M., Berger, F., Briginshaw, L.N., Carella, P., Aguilar-Cruz, A., Davies, K.M., Dierschke, T., Dolan, L., Zachgo, S., 2022. The renaissance and enlightenment of *Marchantia* as a model system. Plant Cell 34, 3512–3542. https://doi.org/10.1093/plcell/koac219.

Branquinho, C., Brown, D.H., 1994. A method for studying the cellular location of lead in lichens. Lichenologist 26 (1), 83–90. https://doi.org/10.1006/lich.1994.1007.

Brown, D., Brown, R., 1991. Mineral cycling and lichens: the physiological basis. Lichenologist 23 (3), 293–307. https://doi.org/10.1017/S0024282991000440.

Brunetti, P., Zanella, L., de Paolis, A., di Litta, D., Cecchetti, V., Falasca, G., Barbieri, M., Altamura, M.M., Costantino, P., Cardarelli, M., 2015. Cadmium-inducible expression

of the ABC-type transporter AtABCC3 increases phytochelatin-mediated cadmium tolerance in Arabidopsis. J. Exp. Bot. 66 (13), 3815–3829. https://doi.org/10.1093/jxb/erv185.

Clemens, S., 2006. Evolution and function of phytochelatin synthases. J. Plant Physiol. 163 (3), 319–332. https://doi.org/10.1016/j.jplph.2005.11.010.

Clemens, S., Aarts, M.G.M., Thomine, S., Verbruggen, N., 2013. Plant science: the key to preventing slow cadmium poisoning. Trends Plant Sci. 18 (2), 92–99. https://doi.org/10.1016/J.TPLANTS.2012.08.003.

Degola, F., Sanità di Toppi, L., Petraglia, A., 2022. Bryophytes: how to conquer an alien planet and live happily (ever after). J. Exp. Bot. 73, 4267–4272. https://doi.org/10.1093/jxb/erac252.

Delalande, O., Desvaux, H., Godat, E., Valleix, A., Junot, C., Labarre, J., Boulard, Y., 2010. Cadmium – glutathione solution structures provide new insights into heavy metal detoxification. FEBS J. 277 (24), 5086–5096. https://doi.org/10.1111/J.1742-4658.2010.07913.X.

Fasani, E., Li, M., Varotto, C., Furini, A., DalCorso, G., 2022. Metal detoxification in land plants: from bryophytes to vascular plants. State of the art and opportunities. Plants 11 (3), 237. https://doi.org/10.3390/plants11030237.

Foyer, C.H., Noctor, G., 2001. The molecular biology and metabolism of glutathione. Plant Ecophysiology. Springer,, Netherlands, pp. 27–56. https://doi.org/10.1007/0-306-47644-4_3.

Fu, S., Lu, Y., Zhang, X., Yang, G., Chao, D., Wang, Z., Shi, M., Chen, J., Chao, D.Y., Li, R., Ma, J.F., Xia, J., 2019. The ABC transporter ABCG36 is required for cadmium tolerance in rice. J. Exp. Bot. 70 (20), 5909–5918. https://doi.org/10.1093/jxb/erz33.

Giardini, S., Bellini, E., Bandoni, E., Saba, A., Sanità di Toppi, L., 2022. Tools for *in vitro* propagation/synchronization of the liverwort *Marchantia polymorpha* and application of a validated HPLC-ESI-MS-MS method for glutathione and phytochelatin analysis. Stresses 2 (1), 136–145. https://doi.org/10.3390/stresses2010010.

González, A.G., Pokrovsky, O.S., 2014. Metal adsorption on mosses: Toward a universal adsorption model. J. Colloid Interface Sci. 415, 169–178. https://doi.org/10.1016/J.JCIS.2013.10.028.

Grill, E., Winnacker, E.-L., Zenk, M.H., 1985. Phytochelatins: the principal heavy-metal complexing peptides of higher plants. Science 230 (4726), 674–676. https://doi.org/10.1126/science.230.4726.674.

Hwang, T.L., Shaka, A.J., 1998. Multiple-pulse mixing sequences that selectively enhance chemical exchange or cross-relaxation peaks in high-resolution NMR spectra. J. Magn. Reson. 135 (2), 280–287. https://doi.org/10.1006/JMRE.1998.1598.

IAEA, 1995, Survey of reference materials. Volume 1: Biological and environmental reference materials for trace elements, nuclides and microcontaminants. International Atomic Energy Agency, report IAEA-TECDOC-854, Vienna (Austria).

Ishizaki, K., Chiyoda, S., Yamato, K.T., Kohchi, T., 2008. Agrobacterium-mediated transformation of the haploid liverwort *Marchantia polymorpha* L., an emerging model for plant biology. Plant Cell Physiol. 49 (7), 1084–1091. https://doi.org/10.1093/PCP/PCN085.

Ishizaki, K., Johzuka-Hisatomi, Y., Ishida, S., Iida, S., Kohchi, T., 2013. Homologous recombination-mediated gene targeting in the liverwort *Marchantia polymorpha* L. Sci. Rep. 3 (1), 1–6. https://doi.org/10.1038/srep01532.

Ismael, M.A., Elyamine, A.M., Moussa, M.G., Cai, M., Zhao, X., Hu, C., 2019. Cadmium in plants: uptake, toxicity, and its interactions with selenium fertilizers. Metallomics 11, 255. https://doi.org/10.1039/c8mt00247a.

Kim, D.Y., Bovet, L., Maeshima, M., Martinoia, E., Lee, Y., 2007. The ABC transporter AtPDR8 is a cadmium extrusion pump conferring heavy metal resistance. Plant J. 50 (2), 207–218. https://doi.org/10.1111/j.1365-313X.2007.03044.x.

Klein, M., Burla, B., Martinoia, E., 2006. The multidrug resistance-associated protein (MRP/ABCC) subfamily of ATP-binding cassette transporters in plants. FEBS Lett. 580 (4), 1112–1122. https://doi.org/10.1016/J.FEBSLET.2005.11.056.

Kneer, R., Zenk, M.H., 1997. The formation of Cd-phytochelatin complexes in plant cell cultures. Phytochemistry 44 (1), 69–74. https://doi.org/10.1016/S0031-9422(96)00514-6.

Kobae, Y., Sekino, T., Yoshioka, H., Nakagawa, T., Martinoia, E., Maeshima, M., 2006. Loss of AtPDR8, a plasma membrane ABC transporter of *Arabidopsis thaliana*, causes hypersensitive cell death upon pathogen infection. Plant Cell Physiol. 47 (3), 309–318. https://doi.org/10.1093/pcp/pcj001.

Kubier, A., Wilkin, R.T., Pichler, T., 2019. Cadmium in soils and groundwater: A review. Appl. Geochem. 108, 104388 https://doi.org/10.1016/J.APGEOCHEM.2019.104388.

Kubota, A., Ishizaki, K., Hosaka, M., Kohchi, T., 2013. Efficient agrobacterium-mediated transformation of the liverwort *Marchantia polymorpha* using regenerating thalli. Biosci., Biotechnol., Biochem. 77 (1), 167–172. https://doi.org/10.1271/bbb.120700.

Lazo, P., Bekteshi, L., Shehu, A., 2013. Active moss biomonitoring technique for atmospheric deposition of heavy metals in Elbasan city, Albania. Fresenius Environ. Bull. 22 (1), 8.

Li, M., Barbaro, E., Bellini, E., Saba, A., Sanità di Toppi, L., Varotto, C., 2020. Ancestral function of the phytochelatin synthase C-terminal domain in inhibition of heavy metal-mediated enzyme overactivation. J. Exp. Bot. 71 (20), 6655–6669. https://doi.org/10.1093/JXB/ERAA386.

Livak, K.J., Schmittgen, T.D., 2001. Analysis of relative gene expression data using real-time quantitative PCR and the $2^{-\Delta\Delta CT}$ method. Methods 25 (4), 402–408. https://doi.org/10.1006/meth.2001.1262.

Maresca, V., Sorbo, S., Loppi, S., Funaro, F., del Prete, D., Basile, A., 2020. Biological effects from environmental pollution by toxic metals in the "land of fires" (Italy) assessed using the biomonitor species *Lunularia cruciata* L. (Dum). Environ. Pollut. 265, 115000 https://doi.org/10.1016/J.ENVPOL.2020.115000.

Martinoia, E., 2018. Vacuolar Transporters – Companions on a longtime journey. Plant Physiol. 176, 1384–1407. https://doi.org/10.1104/pp.17.01481.

Mautsoe, P.J., Beckett, R.P., 1996. A preliminary study of the factors affecting the kinetics of cadmium uptake by the liverwort *Dumortiera hirsuta*, 1996 S. Afr. J. Bot. 62 (6), 332–336. https://doi.org/10.1016/s0254-6299(15)30675-x.

Meyer, C.L., Peisker, D., Courbot, M., Craciun, A.R., Cazalé, A.C., Desgain, D., Schat, H., Clemens, S., Verbruggen, N., 2011. Isolation and characterization of *Arabidopsis halleri* and *Thlaspi caerulescens* phytochelatin synthases. Planta 234, 83–95. https://doi.org/10.1007/s00425-011-1378-z.

Morris, J.L., Puttick, M.N., Clark, J.W., Edwards, D., Kenrick, P., Pressel, S., Wellman, C.H., Yang, Z., Schneider, H., Donoghue, P.C.J., 2018. The timescale of early land plant evolution. Proc. Natl. Acad. Sci. U. S. A. 115 (10), E2274–E2283. https://doi.org/10.1073/PNAS.1719588115.

Orwar, O., Fishman, H.A., Ziv, N.E., Scheller, R.H., Zare, R.N., 1995. Use of 2,3-Naphthalenedicarboxaldehyde derivatization for single-cell analysis of glutathione by capillary electrophoresis and histochemical localization by fluorescence microscopy. Anal. Chem. 67 (23), 4261–4268. https://doi.org/10.1021/ac00119a010.

Park, J., Song, W.Y., Ko, D., Eom, Y., Hansen, T.H., Schiller, M., Lee, T.G., Martinoia, E., Lee, Y., 2012. The phytochelatin transporters AtABCC1 and AtABCC2 mediate tolerance to cadmium and mercury. Plant J. 69 (2), 278–288. https://doi.org/10.1111/j.1365-313X.2011.04789.x.

Pence, N.S., Larsen, P.B., Ebbs, S.D., Letham, D.L.D., Lasat, M.M., Garvin, D.F., Eide, D., Kochian, L., 2000. The molecular physiology of heavy metal transport in the Zn/Cd hyperaccumulator *Thlaspi caerulescens*. Proc. Natl. Acad. Sci. U. S. A. 97 (9), 4956–4960. https://doi.org/10.1073/PNAS.97.9.4956.

Pérez-Llamazares, A., Galbán-Malagón, C.J., Aboal, J.R., Angel Fernández, J., Carballeira, A., 2010. Evaluation of cations and chelating agents as extracellular extractants for Cu, Pb, V and Zn in the sequential elution technique applied to the terrestrial moss *Pseudoscleropodium purum*. Ecotoxicol. Environ. Saf. 73, 507–514. https://doi.org/10.1016/j.ecoenv.2009.12.019.

Pfeifer, L., Mueller, K.K., Classen, B., 2022. The cell wall of hornworts and liverworts: innovations in early land plant evolution? J. Exp. Bot. 73, 4454–4472. https://doi.org/10.1093/jxb/erac157.

Połeć-Pawlak, K., Ruzik, R., Lipiec, E., 2007. Investigation of Cd(II), Pb(II) and Cu(I) complexation by glutathione and its component amino acids by ESI-MS and size exclusion chromatography coupled to ICP-MS and ESI-MS. Talanta 72 (4), 1564–1572. https://doi.org/10.1016/j.talanta.2007.02.008.

Procko, E., O'Mara, M.L., Bennett, W.F.D., Tieleman, D.P., Gaudet, R., 2009. The mechanism of ABC transporters: general lessons from structural and functional studies of an antigenic peptide transporter. FASEB J. 23 (5), 1287–1302. https://doi.org/10.1096/FJ.08-121855.

Renzaglia, K.S., Aguilar, J.C.V., Garbary, D.J., 2018. Morphology supports the setaphyte hypothesis: mosses plus liverworts form a natural group. Bryophyt. Divers. Evol. 40 (2), 11–17–11–17. https://doi.org/10.11646/BDE.40.2.1.

Ross, H.B., 1990. On the use of mosses (*Hylocomium splendens* and *Pleurozium schreberi*) for estimating atmospheric trace metal deposition. Water, Air, Soil Pollut. 50 (1), 63–76. https://doi.org/10.1007/BF00284784.

Saint-Marcoux, D., Proust, H., Dolan, L., Langdale, J.A., 2015. Identification of reference genes for Real-Time quantitative PCR experiments in the liverwort *Marchantia polymorpha*. PLOS ONE 10 (3), e0118678. https://doi.org/10.1371/JOURNAL.PONE.0118678.

Salt, D.E., Rauser, W.E., 1995. MgATP-dependent transport of phytochelatins across the tonoplast of oat roots. Plant Physiol. 107 (4), 1293–1301. https://doi.org/10.1104/PP.107.4.1293.

Sanità di Toppi, L., Gabbrielli, R., 1999. Response to cadmium in higher plants. Environ. Exp. Bot. 41 (2), 105–130. https://doi.org/10.1016/S0098-8472(98)00058-6.

Schafer, F.Q., Buettner, G.R., 2001. Redox environment of the cell as viewed through the redox state of the glutathione disulfide/glutathione couple. Free Radic. Biol. Med. 30 (11), 1191–1212. https://doi.org/10.1016/S0891-5849(01)00480-4.

Schröder, P., Collins, C., 2002. Conjugating enzymes involved in xenobiotic metabolism of organic xenobiotics in plants. Int. J. Phytoremediat. 4 (4), 247–265. https://doi.org/10.1080/15226510208500086.

Sharma, S., 2007. *Marchantia polymorpha* L.: A Bioaccumulator. Aereobiologia 23, 181–187. https://doi.org/10.1007/s10453-007-9062-2.

Shimamura, M., 2016. *Marchantia polymorpha*: Taxonomy, phylogeny and morphology of a model system. Plant Cell Physiol. 57 (2), 230–256. https://doi.org/10.1093/pcp/pcv192.

Song, W.Y., Park, J., Mendoza-Cózatl, D.G., Suter-Grotemeyer, M., Shima, D., Hörtensteiner, S., Geisler, M., Weder, B., Rea, P.A., Rentsch, D., Schroeder, J.I., Lee, Y., Martinoia, E., 2010. Arsenic tolerance in Arabidopsis is mediated by two ABCC-type phytochelatin transporters. Proc. Natl. Acad. Sci. 107 (49), 21187–21192. https://doi.org/10.1073/PNAS.1013964107.

Song, W.Y., Park, J., Eisenach, C., Maeshima, M., Lee, Y., Martinoia, E., 2014. ABC Transporters and Heavy Metals. Plant ABC Transporters. Springer,, Netherlands, pp. 1–17. https://doi.org/10.1007/978-3-319-06511-3_1.

Sorrentino, M., Capozzi, F., Amitrano, C., de Tommaso, G., Arena, C., Iuliano, M., Giordano, S., Spagnuolo, V., 2021. Facing metal stress by multiple strategies: morphophysiological responses of cardoon (*Cynara cardunculus* L.) grown in hydroponics. Environ. Sci. Pollut. Res. 28, 37616–37626. https://doi.org/10.1007/s11356-021-13242-9.

Spagnuolo, V., Zampella, M., Giordano, S., Adamo, P., 2011. Cytological stress and element uptake in moss and lichen exposed in bags in urban area. Ecotoxicol. Environ. Saf. 74 (5), 1434–1443. https://doi.org/10.1016/J.ECOENV.2011.02.011.

Speiser, D.M., Abrahamson, S.L., Banuelos, G., Ow, D.W., 1992. *Brassica juncea* produces a phytochelatin-cadmium-sulfide complex. Plant Physiol. 99 (3), 817–821. https://doi.org/10.1104/PP.99.3.817.

Stanković, J.D., Sabovljević, A.D., Sabovljević, M.S., 2018. Bryophytes and heavy metals: A review. Acta Bot. Croat. 77 (2), 109–118. https://doi.org/10.2478/botcro-2018-0014.

Sterckeman, T., Thomine, S., 2020. Mechanisms of cadmium accumulation in plants. Crit. Rev. Plant. Sci. 39 (4), 322–359. https://doi.org/10.1080/07352689.2020.1792179.

Sugano, S.S., Shirakawa, M., Takagi, J., Matsuda, Y., Shimada, T., Hara-Nishimura, I., Kohchi, T., 2014. CRISPR/Cas9-mediated targeted mutagenesis in the liverwort *Marchantia polymorpha* L. Plant Cell Physiol. 55 (3), 475–481. https://doi.org/10.1093/pcp/pcu014.

Tyler, G., 1990. Bryophytes and heavy metals: a literature review. Bot. J. Linn. Soc. 104 (1–3), 231–253. https://doi.org/10.1111/j.1095-8339.1990.tb02220.x.

Uraguchi, S., Nagai, K., Naruse, F., Otsuka, Y., Ohshiro, Y., Nakamura, R., Takanezawa, Y., Kiyono, M., 2021. Development of affinity bead-based *in vitro* metal-ligand binding assay reveals dominant cadmium affinity of thiol-rich small peptides phytochelatins beyond glutathione. Metallomics 13, mfab068. https://doi.org/10.1093/mtomcs/mfab068.

Vögeli-Lange, R., Wagner, G.J., 1990. Subcellular localization of cadmium and cadmium-binding peptides in tobacco leaves. Plant Physiol. 92, 1086–1093 https://doi.org/10.1104%2Fpp.92.4.1086.

Vögeli-Lange, R., Wagner, G.J., 1996. Relationship between cadmium, glutathione and cadmium-binding peptides (phytochelatins) in leaves of intact tobacco seedlings. Plant Sci. 114, 11–18. https://doi.org/10.1016/0168-9452(95)04299-7.

Wanke, D., Kolukisaoglu, H., 2010. An update on the ABCC transporter family in plants: Many genes, many proteins, but how many functions? Plant Biol. 12 (1), 15–25. https://doi.org/10.1111/j.1438-8677.2010.00380.x.

Yang, L., Nadeau, K., Grinberg, P., Brophy, C., Gedara, I.P., Meija, J., Mester, Z., Willie, S., McRae, G., 2015, SLRS-6 certified values for the mass fraction and concentration of trace metals and other constituents. Ottawa: National Research Council, Canada. https://doi.org/10.4224/crm.2015.slrs-6.

Zeng, F., Chen, G., Chen, X., Li, Q., Wu, X., Zhang, G., 2020. Cadmium accumulation in plants: Insights from physiological/molecular mechanisms to evolutionary biology. Authorea. https://doi.org/10.22541/AU.159665033.36792189.

Zenk, M.H., 1996. Heavy metal detoxification in higher plants - a review. Gene 179 (1), 21–30. https://doi.org/10.1016/S0378-1119(96)00422-2.

Li, M., Leso, M., Buti, M., Bellini, E., Bertoldi, D., Saba, A., Larcher, R., Sanità di Toppi, L., Varotto, C., 2022. Phytochelatin synthase de-regulation in *Marchantia polymorpha* indicates cadmium detoxification as its primary ancestral function in land plants and provides a novel visual bioindicator for detection of this metal. J. Hazard. Mater. 440, 129844. https://doi.org/10.1016/j.jhazmat.2022.129844.